

Time-resolved analysis of fMRI signal changes using Brain Activation Movies

Christian Windischberger^{a,b}, Ross Cunnington^c, Claus Lamm^d, Rupert Lanzenberger^e,
Herbert Langenberger^f, Lüder Deecke^g, Herbert Bauer^d, Ewald Moser^{a,b,f,h,*}

^a MR Center of Excellence, Medical University of Vienna, Lazarettgasse 14,
A-1090 Vienna, Austria

^b Center for Biomedical Engineering and Physics, Medical University of Vienna, Austria

^c Howard-Florey-Institute, University of Melbourne, Australia

^d Brain Research Lab, Department of Psychology, University of Vienna, Austria

^e Department of Psychiatry and Psychotherapy, Medical University of Vienna, Austria

^f Department of Radiology, Medical University of Vienna, Austria

^g Department of Neurology, Medical University of Vienna, Austria

^h Department of Psychiatry, University of Pennsylvania, Philadelphia, USA

Received 16 September 2007; received in revised form 27 November 2007; accepted 29 November 2007

Abstract

Conventional fMRI analyses assess the summary of temporal information in terms of the coefficients of temporal basis functions. Based on established finite impulse response (FIR) analysis methodology we show how spatiotemporal statistical parametric maps may be concatenated to form Brain Activation Movies (BAMs), dynamic activation maps representing the temporal evolution of brain activation throughout task performance. These BAMs enable comprehensive assessment of the dynamics in functional topology without restriction to predefined regions and without detailed information on the stimulus paradigm. We apply BAM visualization to two fMRI studies demonstrating the additional spatiotemporal information available compared to standard fMRI result presentation. Here we show that BAMs allow for unbiased data visualization providing dynamic activation maps without assumptions on the neural activity except reproducibility across trials. It may thus be useful in proceeding from static to dynamic brain mapping, widening the range of fMRI in neuroscience. In addition, BAMs might be helpful tools in visualizing the temporal evolution of activation in “real-time” for better and intuitive understanding of temporal processes in the human brain.

© 2007 Elsevier B.V. All rights reserved.

Keywords: fMRI; Topology; Motor; Cognition; Mental rotation

1. Introduction

In fMRI analyses performed with validated software packages (e.g. SPM, FSL, fmristat, AFNI, BrainVoyager) temporal parameters of the haemodynamic response are most often accounted for during model estimation by using carefully designed temporal basis functions. The overwhelming number of published studies does not, however, explicitly target the temporal dimension of fMRI, restricting analysis results to non-

dynamic brain activation maps during different experimental conditions.

On the other hand, studies assessing fMRI activation dynamics typically extract time courses from predefined regions of interest and assess temporal parameters, such as activation onsets and durations, from those time courses. In particular, studies on mental chronometry have used temporal fMRI signal parameters to examine interregional activation characteristics via time-resolved fMRI (Menon et al., 1998; Richter et al., 2000; Weilke et al., 2001). These studies were, however, limited to predefined brain regions, from which activation onsets and durations were calculated.

A different approach to display activation dynamics is to perform repeated correlation of fMRI signal changes with

* Corresponding author at: MR Center of Excellence, Medical University of Vienna, Lazarettgasse 14, A-1090 Vienna, Austria. Tel.: +43 1 40400 3773; fax: +43 1 40400 7631.

E-mail address: ewald.moser@meduniwien.ac.at (E. Moser).

time-shifted versions of either boxcar functions (Wildgruber et al., 1997) or the expected haemodynamic response (Cunnington et al., 2003; Hulsmann et al., 2003). Although such an analysis approach can reach a temporal sensitivity of a few hundred milliseconds (Hernandez et al., 2002), it relies on predefined response functions which are most often based on a presumed neural activity pattern convolved with an expected haemodynamic response function to account for the physiological coupling of neural activity and vascular changes (Friston et al., 1995).

Friston et al. suggested the use of temporal derivatives of the expected haemodynamic response as additional regressors in the general linear model (GLM) as an elegant way to allow for differential latencies among brain areas (Friston et al., 1998). Differences in these temporal derivatives can then be used to make statistical inferences about the timing of activation between conditions (Cunnington et al., 2002). Although this method enables a straightforward assessment of temporal parameters, it requires very strong assumptions on the expected signal changes and will obviously fail if the actual brain activity differs from what is anticipated. Even more, the haemodynamic response function (HRF) itself has been shown to vary considerably between subjects and brain regions (Aguirre et al., 1998; Cunnington et al., 2003; Duann et al., 2002; Handwerker et al., 2004; Lee et al., 1995) which might render temporal parameters derived from analysis with a canonical HRF erroneous.

With reduced requirements for detailed model specification, finite impulse response (FIR) approaches represent tools for calculating unbiased and statistically efficient estimates of the underlying haemodynamic responses associated with event-related fMRI experiments (Boynton et al., 1996; Burock and Dale, 2000; Dale and Buckner, 1997; Ollinger et al., 2001a; Wildgruber et al., 2002). In FIR analysis signal changes are generally modeled by a set of orthogonal basis functions which can fit and describe a wide range of possible time courses. As a result, separate activation maps are obtainable for each time instance within a trial. FIR methodology is readily implemented in many fMRI analysis software packages and forms the basis for the concept presented in this paper. Previous applications of FIR analyses have used *F*-tests over all regressors to calculate static statistical maps (Burock and Dale, 2000). Such approaches reveal voxels which show significant signal differences over the whole experiment. Here we calculate separate statistical parametric maps for each FIR regressor and concatenate these maps into a 4D matrix representing the temporal evolution of brain activation in every voxel of the data set. Each map reflects activation at a specific time instance after trial onset. Replaying these activation maps at a frame rate similar to the acquisition rate yields an animated Brain Activation Movie (BAM) visualizing the temporal evolution of brain activation in “real-time” for the whole data set without restriction to certain ROIs (see BAMs provided as Supplementary material).

We apply the BAM visualization approach in two fMRI experiments demonstrating the additional information and novel insights gained. The first experiment examines the temporal characteristics of brain activation on a single subject basis during externally cued finger movements, in particular investigating

activation in M1 and SMA. In the second experiment we extend the BAM technique to second-level random effects group analysis showing the temporal evolution of fronto-parietal activity in a cognitive paradigm where 12 subjects had to decide whether their mental representation of a geometric object was identical to a presented stimuli, a task requiring visual imagery and mental rotation.

2. Materials and methods

FIR analysis with BAM visualization can be implemented easily within the common GLM-based analysis packages (SPM, FSL, fmristat, AFNI, BrainVoyager). It involves creating a model with a series of non-overlapping box-car regressors at each TR interval around the time of each stimulus event. In estimating the model, these box-car regressors are fitted to the actual BOLD response occurring around the time of each stimulus event. Maps of activation at each TR interval relative to the stimulus event can then be obtained by specifying a series of *t*-contrasts individually for each box-car regressor. As such, there are no assumptions on the individual HRF or even the underlying neuronal activity other than reproducibility across repeated trials, i.e. arbitrary time courses after trial onset can be modeled appropriately.

2.1. fMRI study I: motor paradigm

A group of six subjects (three male, three female; mean age: 24a) without a history of neurological or psychiatric disorders participated in this study. The study was approved by the local ethics committee and all subjects gave written informed consent prior to participation. All subjects were right-handed according to the Edinburgh handedness inventory (Oldfield, 1971).

Measurements were performed on a 3 Tesla Medspec scanner (Bruker Biospin, Germany) using gradient-recalled EPI. Four axial slices of 5 mm thickness (1 mm gap) were acquired with a matrix size of 64×64 voxels, a TE of 40 ms and a TR of 300 ms. Voxel size was 2.96×2.96 mm. Slices were positioned to cover the primary motor cortex (M1), the lateral premotor (PM) areas and the supplementary motor area (SMA). The very short TR was chosen to ensure appropriate coverage of the haemodynamic response. In each of the 12 trials the subjects listened via headphones to a voice that counted down from “10” to “0” and back to “5”. Subjects were asked to closely attend to the countdown and perform a brief finger movement as soon as they heard “0”. The movement consisted of three brief button-presses with the index-middle-index finger of the right hand. Subjects were instructed to perform these movements as rapidly as possible. Following each trial there was a pause of 18 s which allowed the haemodynamic response to return to baseline. Accordingly, each trial lasted 33 s (110 time instances) and during the 12 trials a total of 1320 part-brain images were acquired per subject. Also, T1-weighted images were acquired using a 3D-MDEFT sequence to allow for definition of ROIs.

Data sets were slice timing corrected within SPM. To ensure all four acquired slices are available for analysis, only two-dimensional motion correction was performed using the FSL

software package (<http://www.fmrib.ox.ac.uk/fsl/>). As the last step of preprocessing data were spatially smoothed with an isotropic Gaussian kernel of 6 mm FWHM with SPM. Due to the reduced cortical coverage common to all six subjects (only four slices were acquired) fMRI data were not normalized to standard stereotactic space and analysis was performed on a single subject basis exclusively.

A set of 110 non-overlapping regressors was constructed covering each TR interval (300 ms duration) from the onset of the countdown to the onset of the next countdown. The first box-car regressor had “1” on the first TR interval of each trial (0–300 ms relative to countdown onset) and “0” for all other time points. All other regressors were then generated by progressively shifting the first regressor by one TR interval, thereby covering every 300 ms time interval with sequential but non-overlapping box-car regressors. This set of regressors was used to construct a design matrix in SPM and contrast images for each regressor were calculated. Single subject activation maps were thresholded at a t -value of 4.5 ($p < 0.05$, FWE corrected) and overlaid to an unsaturated echo-planar image. These activation maps were then concatenated to yield a single BAM per subject.

To allow group inferences, ROIs were defined for M1 contralateral to the side of movement execution and for the SMA. Mean time courses were calculated per subject and scaled to a maximum value of 1 before averaging across subjects to enable a direct comparison of the temporal activation features in M1 and SMA.

2.2. fMRI study II: mental rotation paradigm

For this experiment a group of 12 healthy male subjects (mean age: 25a) was recruited. The study was approved by the local ethics committee and all subjects gave written informed consent before participation. All subjects had normal or corrected to normal vision and were right-handed according to a modified version of the Annett handedness inventory (Annett, 1985). Stimuli were presented via a video beamer that projected to a screen positioned behind the subjects which was visible via a small mirror mounted on the head coil.

Each trial consisted of three parts—encoding, mental rotation, and comparison periods (see Fig. 1). Trials began with a

2 s encoding period during which an abstract, two-dimensional object was presented in an arbitrary orientation and subjects were required to memorize the object’s geometric features and its orientation. Following the 2 s encoding period, one edge of the object was indicated by a red bar for 1 s. The screen was then blanked and the object replaced by a fixation cross for 5 s duration. During this period subjects were required to mentally rotate the encoded object so that it should stand on the edge that was indicated by the red bar. After 5 s a test object was presented which was either an identical or horizontally mirrored version of the original object. Subjects were then required to compare the presented object with their mental image of the rotated original object and were given 2 s to respond by pressing one of two buttons with the right index finger on a panel mounted on the right thigh, indicating whether the test object was the same or mirror-reversed compared with the original object. The subject’s response caused the object to immediately disappear from the screen. A rest period varying randomly between 8 and 12 s duration followed each trial, allowing the haemodynamic response to return to baseline before presentation of the next trial. Thirty-two trials were presented per subject leading to a total run time of approximately 10 min.

This study was performed on a 3 Tesla Medspec scanner (Bruker Biospin, Germany), using a gradient-recalled EPI sequence with a matrix size of 64×64 voxels and a FOV of $210 \text{ mm} \times 250 \text{ mm}$, leading to a voxel size of $3.3 \text{ mm} \times 3.9 \text{ mm}$. Six axial slices with a thickness of 4 mm (1 mm gap) were positioned to cover PM, SMA and M1 areas and the superior part of the parietal lobe. Slices were tilted to be approximately parallel to the line connecting the anterior and posterior commissure. One thousand nine hundred and four image slabs were acquired at a TE of 30 ms with a repetition time TR of 350 ms.

Reconstructed images were corrected for slice timing effects and motion artifacts, as well as transformed to standard space using SPM, where spatial smoothing with an isotropic Gaussian kernel of 9 mm FWHM was also performed. Regressors for the FIR analysis were constructed for each subject using timing information recorded during the functional runs. The shortest trial had a length of 18 s, corresponding to 51 image slabs acquired. Accordingly, the SPM design matrix was formed

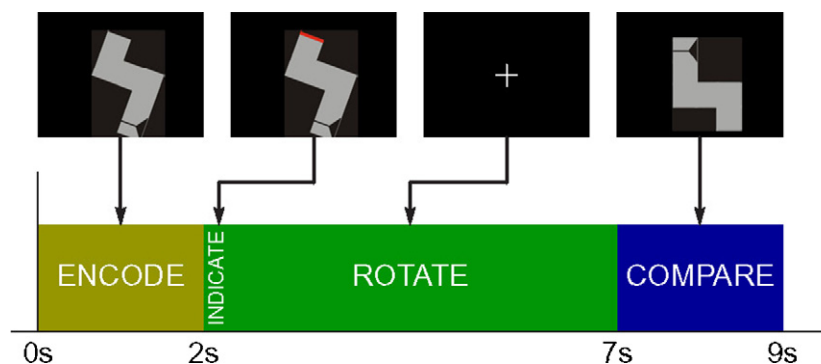


Fig. 1. Stimulation paradigm used in study II. After a geometrical object was presented for a 2 s encoding period one edge was highlighted indicating the final rotation position. Then the screen was blanked for 5 s and subjects were required to perform the mental rotation. Finally, an object was presented for comparison and subjects responded by button-press. (For interpretation of the references to colour in this figure legend, the reader is referred to the web version of the article.)

by 51 regressors, each with only a single time instance per trial being a non-zero value. After parameter estimation contrast images were calculated for each regressor and were entered to a random effects analysis over all 12 subjects. The resulting group activation maps were thresholded at a t -value of 5.4 ($p = 0.0001$, uncorrected) and concatenated to form a BAM of trial-related activity over the whole group studied.

3. Results

3.1. Study I: motor paradigm

For each of the six subjects studied a sequence of 110 activation maps was calculated and combined to gain a BAM. Fig. 2 displays 9 out of 110 maps from a single subject. Because of limited space every third frame is shown only, i.e. the time period between subsequent maps is 900 ms. The complete BAM giving a comprehensive, real-time representation of brain activation is available as [Supplementary material](#). Next to the activation maps in Fig. 2 the corresponding time with respect to movement execution is given. In the uppermost map (2.4 s after movement) activation in the SMA is clearly visible. In fact the onset of this SMA activity occurs concomitantly with the start of the auditory countdown (shifted by the haemodynamic delay) and remains rather constant throughout the movement preparation period (cp. Figs. 3 and 4). At 3.3 s after movement execution SMA activation increases considerably with only sparse activation in M1. Three TRs later, i.e. 4.2 s after movement, SMA activation approaches its peak value, while activity in M1 is just beginning to rise. The maximum M1 activation level for this particular subject is reached at 6.2 s after movement onset.

In Fig. 3 we show BAM data from the same subject, presenting the evolution of brain activation (i.e. 4D data) in a single figure. We have limited our display to a single slice (slice 3) containing both SMA and M1. Closer inspection of the activation maps in Fig. 2 shows that projecting the BAM data along anterior–posterior lines still allows discrimination of SMA and M1 activation, as there is no spatial overlap in this direction. Mean activation was therefore calculated along sagittal lines for all 110 BAM activation maps, resulting in the lower part of Fig. 3 which we denote as a BAM plane. The position in left–right direction is shown on the horizontal axis, with chain-dotted lines indicating M1 and SMA areas. The temporal evolution of brain activation can be observed in vertical direction, the numbers giving the time with respect to movement execution. Green lines mark the start of the auditory cue and the onset of movement, respectively. Similar to Fig. 2 it can be seen that significant SMA activation occurs early within a trial, about 10 s before reaching its maximum. This indicates preparatory activity in the SMA immediately after countdown onset. Fig. 3 also shows a clear differentiation of peak SMA and M1 activities (green arrows), superior to the standard display as seen in Fig. 2.

As mentioned before, Figs. 2 and 3 show BAM results from a single subject without spatial normalization. To still allow group inferences, ROIs of SMA and M1 were defined in all six subjects and mean time courses were calculated. The results of this ROI

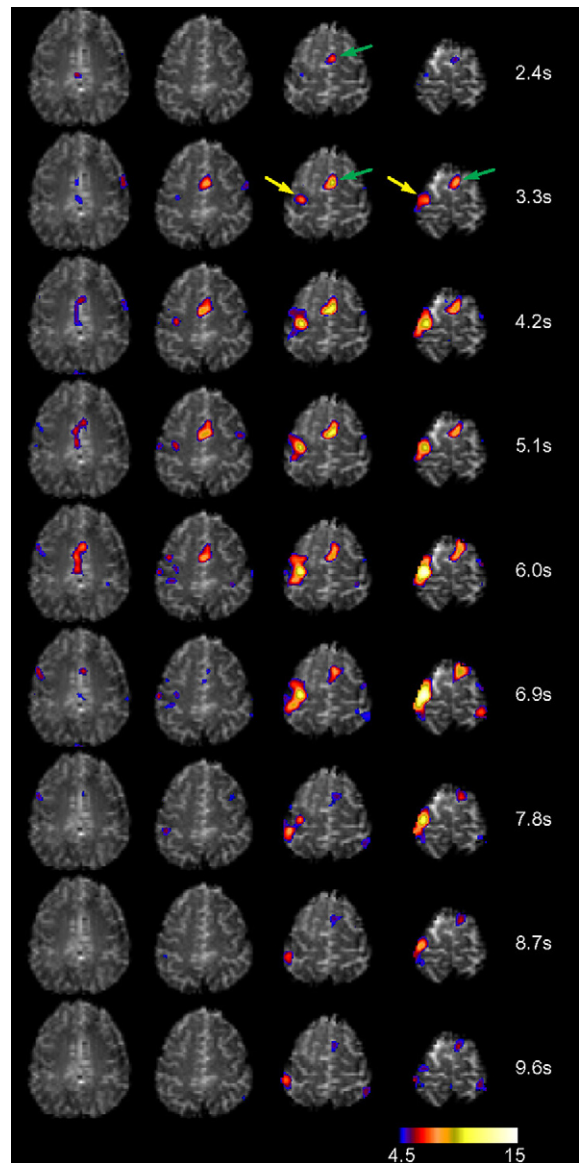


Fig. 2. BAM in a single subject performing a cued movement (study I) overlaid on a high-resolution echo planar image. Subsequent BAM frames show the dynamic spatio-temporal pattern of functional activation during preparation and execution of movement. Note that every third frame is shown only, i.e. the time period between frames is 900 ms. The complete movie encompassing all 110 BAM frames is available as [Supplementary material](#). Numbers indicate the time delay from movement execution. BAM analysis shows an early signal increase in the SMA (green arrows) which is followed by activation in M1 (yellow arrows). (For interpretation of the references to colour in this figure legend, the reader is referred to the web version of the article.)

analysis in terms of mean and standard error can be seen in Fig. 4. It is apparent that both ROI time courses exhibit a high degree of baseline stability, both before cue onset and after movement execution. In concordance with the single subject results the early onset of SMA activation (grey line) is consistently observable across all subjects studied. As suggested in Figs. 2 and 3 the activation peak in the SMA clearly precedes M1 activation. Averaged across the group the timing difference was calculated to be 0.9 s.

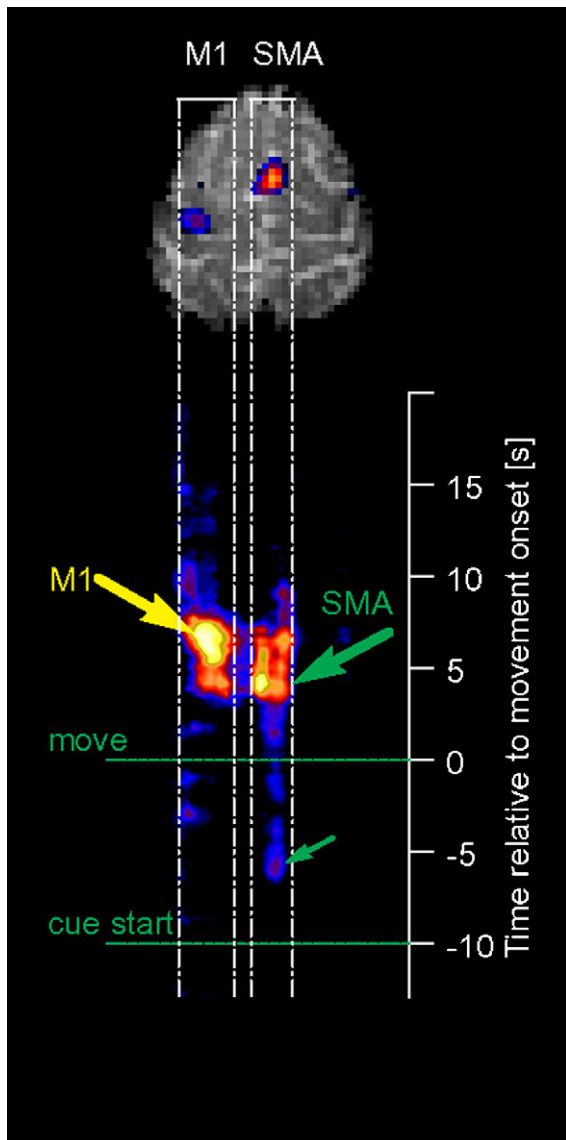


Fig. 3. Single BAM plane showing the temporal evolution of brain activation (same subject as in Fig. 2). For each BAM frame activation in slice 3 (upper part) is projected in anterior–posterior direction forming a BAM plane. Time is given relative to movement execution, and countdown start and movement execution are indicated with dashed green lines. It can be seen that SMA activates immediately (thin green arrow, shifted by the haemodynamic delay) after the cue onset and remains activated at a constant level for the whole countdown period, but increases considerably (thick green arrow) shortly before movement execution, reaching its maximum approximately 1 s before maximum M1 activation occurs (yellow arrow). (For interpretation of the references to colour in this figure legend, the reader is referred to the web version of the article.)

3.2. Study II: mental rotation

FIR analysis yielded a set of 51 activation maps per subject—each map reflecting the activation pattern at a specified time point after trial onset. These were entered into a random-effects group analysis to examine the temporal evolution of brain activation within a trial period across all 12 subjects. This group BAM consists of 51 separate group analyses, each reflecting common activation patterns at a single time point after trial start. The complete BAM depicting real-

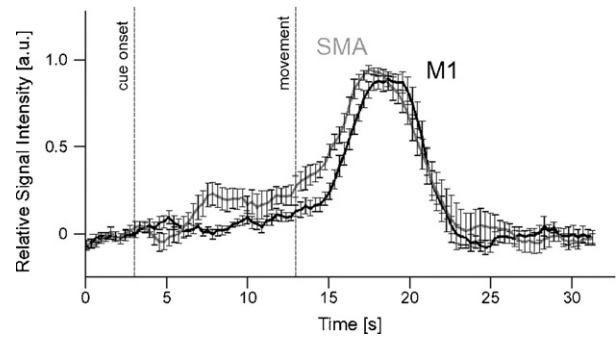


Fig. 4. Time courses in SMA and M1 regions averaged across all six subjects. Note that time courses were normalized per subject to a maximum value of 1 before averaging to allow a direct comparison of SMA (grey) and M1 activation (black). Error bars indicate standard errors. Early SMA activation associated with the onset of the auditory cue is present throughout the countdown period and increases due to final movement preparation processes. Across subjects peak M1 activation occurs 0.9 s after maximum SMA activation reflecting the BOLD-equivalent of the cortical readiness potential frequently found in electrophysiology.

time brain activation topology is provided as [Supplementary material](#).

Because of limited space only a single axial BAM slice ($z=60$ mm) is shown over trial time in Fig. 5, overlaid on the SPM T1-weighted canonical image. The corresponding time after trial onset is given in the lower left corner of each image and the image background is color-coded according to the different processing steps (stimulus encoding, yellow; rotation, green; comparison/response, blue; see Fig. 1) and shifted by 3 s to account for the haemodynamic response delay. Transitions between the distinct processing steps are displayed smoothly (four time points; 1.4 s) to provide for individual differences in the HRF.

Initial activation is visible bilaterally in the parietal cortex about 2 s after trial onset, spreading to SMA and PM areas shortly thereafter. The strength of this activation pattern increases as processing changes from stimulus encoding to the actual mental rotation step, reaching its maximum at about 6.5 s after stimulus onset. At this point activation in parietal cortex, SMA and PM starts to deplete towards the end of the rotation period (about 9 s post-stimulus onset). With the transition from the rotation condition to the stimulus comparison part (10 s post-stimulus onset) stronger activation in SMA and PM cortex becomes apparent, with activation in left M1 indicating the subjects' response at about 11 s after trial start. Due to the broad haemodynamic response and draining vein effects activation can also be seen well after the actual stimulus end, i.e. succeeding the M1 activation peak. As with study I, activation is limited to the stimulus presentation and processing period. No activated voxels are present at the beginning and the end of the trial, even though no information on the stimulus timing within trials was used during analysis.

4. Discussion

The visualization concept presented here assesses the temporal evolution of brain activation over trials to form Brain

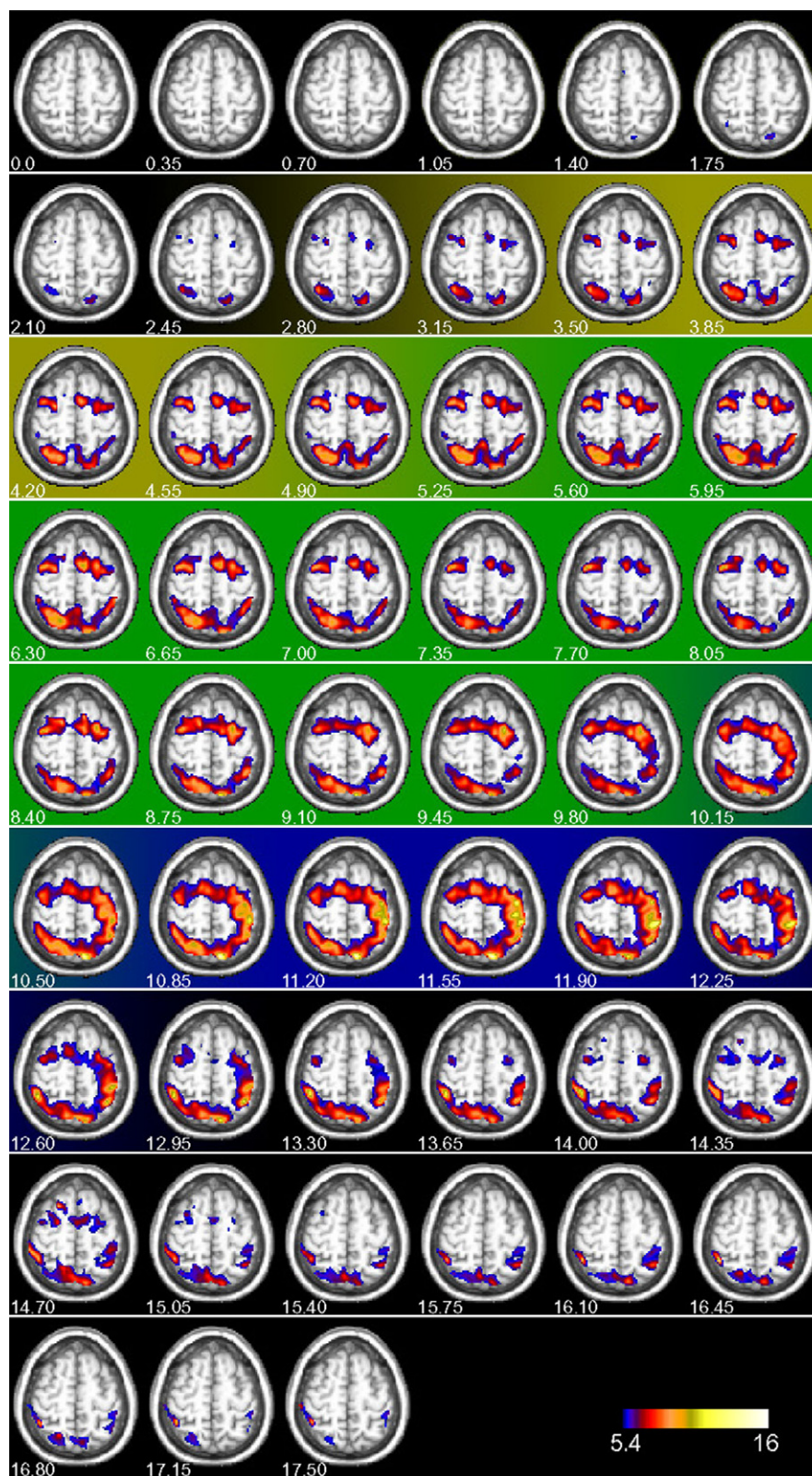


Fig. 5. BAM group analysis results in a single plane. Colors of the image background (extracerebral) correspond to the three different processing steps as described in Fig. 1, shifted by 3 s to account for the haemodynamic delay. Initial stimulus encoding activates a network of cortical areas including the SMA and lateral PM regions which modulates in strength and size during the mental rotation period. In the comparison period strong activation is visible in the left PM area which decreases as SMA and MI activation increases in the advent of responding. The complete BAM is available as Supplemental material. (For interpretation of the references to colour in this figure legend, the reader is referred to the web version of the article.)

Activation Movies, dynamic real-time representations of topological changes in brain activation during stimulus processing. Based on FIR methodology (Dale and Buckner, 1997) trial-locked signal changes are extracted from fMRI data sets without ROI restrictions and without assumptions on the haemodynamic response or the underlying neural activation patterns. This distinguishes the FIR analysis approach from typical strictly model-based analyses with predefined haemodynamic response shapes. It has been demonstrated that latency maps may be obtained based on the pixel-wise fitted BOLD response (Formisano et al., 2002). Such an approach, however, requires a priori model functions to be defined, where deviations of the expected from the actual haemodynamic response may lead to erroneous latency estimates, or even missed activation (Baumgartner et al., 2000; Ollinger et al., 2001b). Model-based analysis is the method of choice when testing of a priori hypotheses is required. With BAMs spatio-temporal characteristics of brain activation can be assessed in an exploratory manner, allowing the study of the temporal sequence in which different areas are activated without prior knowledge or assumptions about BOLD response timing or shape. Such, FIR and model-based techniques are complementary rather than competing methodologies.

In this paper we performed two fMRI studies, one study targeting single subject BAM results, the other aiming at random-effects group BAMs. Both studies presented here were designed to show the potentials of BAM visualization, especially its capability to display the temporal characteristics of brain activation over a trial without restriction to certain ROIs.

Single subject results of study I clearly showed differences in the activation time courses in SMA and M1 during execution of cued finger movements. The calculated temporal delay of 0.9 s is concordant with fMRI studies that report a delay of 0.8 s between SMA and M1 activation (Wildgruber et al., 1997) and EEG studies that show a negative cortical “readiness” occurring 1–2 s prior to predictably cued movements (Cunnington et al., 1995). The increase of SMA activity shortly after the start of the auditory cue is concordant with previous studies reporting SMA activation during the anticipatory interval between a warning and a response-triggering stimulus (Lee et al., 1999; Nagai et al., 2004). From our results SMA activation exhibits constant activation amplitude for about 8 s, i.e. during most of the preparatory cue, before rising to its maximum approximately 1 s before activation peaks in M1. It should be noted that there are no activated voxels at the beginning of the trial despite the fact that no baseline period was defined during GLM specification. Also, activation depletes towards the end of the trial period, indicating sufficient inter-stimulus intervals to allow for the return of the HRF.

Study II results demonstrated the differential involvement of PM, SMA, M1 and parietal areas in object encoding, rotation and comparison, respectively. This group BAM visualization gives a comprehensive overview of the brain areas involved in the different stages of processing. As shown in Fig. 5, a common network is recruited during task processing, including PM, SMA and parietal areas which is excellent concordance with previous studies on mental rotation (Lamm et al., 2001; Richter

et al., 1997; Tagaris et al., 1998; Windischberger et al., 2003). Compared to conventional analysis where only time-averaged brain activation is assessable, with BAM visualization it is now possible to demonstrate that these areas are differently involved in the different stages of processing.

However, one has to be careful when interpreting the relative latency between regional activations because the vast majority of these differences are attributable to haemodynamics whose latencies can differ by several seconds, as opposed to latencies at the neuronal level. A straightforward deduction of activation onsets at the neuronal level is, therefore, hindered by the individual HRF which can vary considerably across regions (e.g. Aguirre et al., 1998). The interpretation of BAM group results may be even more difficult as the HRF has been shown considerable variability across subjects. Within the limits imposed by individual HRFs, BAMs may still allow valuable insights in the temporal pattern of brain activation. This may of particular interest in patients with pathologic haemodynamics.

Also, BAM results enable ROI definition based on functional characteristics rather than relying on anatomical landmarks exclusively. As such, the cardinal problems of anatomical ROI definition including co-registration errors between functional and anatomical images and inter-individual differences in functional topology can be minimized or even avoided. It must be noted that although ROI definition based on BAM results is an elegant way to explore signal changes in an fMRI data set, it is, however, not appropriate to perform statistical analysis on the same data sets based on these ROIs.

In our approach the FIR analysis concept is implemented in the SPM framework, but is also easily available in several other software packages (e.g. fmristat, AFNI, BrainVoyager). FIR analysis with BAM visualization yields significant advantages over purely exploratory data analysis methods regarding statistical inferences as, by definition, model-free analysis techniques like ICA or FCA cannot provide statistical inference on the probability of whether a certain model is valid or not. One particular aspect in characterising evoked responses in fMRI with a FIR model is that we can compute a *t*-statistic for every voxel and every peri-stimulus time bin. We have previously applied this method to show how activation patterns at a precise time instance prior to movement initiation significantly differ between experimental conditions (Cunnington et al., 2006). This contrasts with more conventional (usually more efficient) approaches, which implicitly summarise the temporal dynamics in terms of temporal basis functions based on the stimulus function and the HRF.

The key advantage of representing the evoked response with a separate *t*-value in space and time is that we can build a spatiotemporal SPM. Inferences on these 4D SPMs must account for the fact that the number of multiple comparisons is increased by the number of peri-stimulus bins. Simple Bonferroni correction would be too conservative as individual peri-stimulus data points are not statistically independent (e.g. due to the width of the HRF). Random field theory (RFT) is widely applied to consider such data inherent dependencies in 3D, and has also been generalized to higher dimensions (Worsley et al., 1996, 1999). It has been successfully applied to EEG data to infer on

time-frequency SPMs (Kiebel and Friston, 2004a,b; Kilner et al., 2005). RFT would therefore be the method of choice for providing adjusted p -values for spatiotemporal inference in BAM results, assessing both where and when peak responses were elicited.

In conclusion, BAM visualization based on FIR analysis is a form of exploratory analysis and yields a large number of statistical parametric maps enabling the examination of the temporal evolution of brain activation. Although FIR analysis is not limited to fMRI studies with high temporal resolution, BAMs are most useful with short-TR data sets as dynamic changes in activation can be explored with finer time resolution. With long TR, BAM methodology would be most suited for exploring slow changes in brain activation patterns for long duration tasks. It is a powerful method for visualizing dynamic changes in whole-brain activation patterns over trials or tasks. BAM results potentially provide much more information on the actual neural activity patterns than standard analysis techniques as detection is not limited to *where* activation is located but also *when* this activation occurs. Moreover, they might serve as a basis for defining functional areas for connectivity analyses like dynamic causal modeling (DCM, Friston et al., 2003) or structural equation modeling (SEM, Buchel and Friston, 1997). Therefore, visualization topology dynamics using BAMs might further improve our understanding of the brain's processing strategies by raising new hypotheses that can then be tested for with specific model-driven analysis methods.

Acknowledgements

This study was financially supported by the Austrian Science Fund (FWF P-16669-B02), the Austrian National Bank (OeNB P10943) and the HSJS (1472/2002).

Appendix A. Supplementary data

Supplementary data associated with this article can be found, in the online version, at doi:10.1016/j.jneumeth.2007.11.033.

References

- Aguirre GK, Zarahn E, D'Esposito M. The variability of human, BOLD hemodynamic responses. *Neuroimage* 1998;8:360–9.
- Annett M. Left, right, hand, and brain: the right shift theory. London: Erlbaum; 1985.
- Baumgartner R, Somorjai R, Summers R, Richter W, Ryner L. Correlator beware: correlation has limited selectivity for fMRI data analysis. *Neuroimage* 2000;12:240–3.
- Boynton GM, Engel SA, Glover GH, Heeger DJ. Linear systems analysis of functional magnetic resonance imaging in human V1. *J Neurosci* 1996;16:4207–21.
- Buchel C, Friston KJ. Modulation of connectivity in visual pathways by attention: cortical interactions evaluated with structural equation modelling and fMRI. *Cereb Cortex* 1997;7:768–78.
- Burock MA, Dale AM. Estimation and detection of event-related fMRI signals with temporally correlated noise: a statistically efficient and unbiased approach. *Hum Brain Mapp* 2000;11:249–60.
- Cunnington R, Ianssek R, Bradshaw JL, Phillips JG. Movement-related potentials in Parkinson's disease. Presence and predictability of temporal and spatial cues. *Brain* 1995;118(Pt 4):935–50.
- Cunnington R, Windischberger C, Deecke L, Moser E. The preparation and execution of self-initiated and externally-triggered movement: a study of event-related fMRI. *Neuroimage* 2002;15:373–85.
- Cunnington R, Windischberger C, Deecke L, Moser E. The preparation and readiness for voluntary movement: a high-field event-related fMRI study of the Bereitschafts-BOLD response. *Neuroimage* 2003;20:404–12.
- Cunnington R, Windischberger C, Robinson S, Moser E. The selection of intended actions and the observation of others' actions: a time-resolved fMRI study. *Neuroimage* 2006;29:1294–302.
- Dale AM, Buckner RL. Selective averaging of rapidly presented individual trials using fMRI. *Hum Brain Mapp* 1997;5:329–40.
- Duann JR, Jung TP, Kuo WJ, Yeh TC, Makeig S, Hsieh JC, et al. Single-trial variability in event-related BOLD signals. *Neuroimage* 2002;15:823–35.
- Formisano E, Linden DE, Di Salle F, Trojano L, Esposito F, Sack AT, et al. Tracking the mind's image in the brain I: time-resolved fMRI during visuospatial mental imagery. *Neuron* 2002;35:185–94.
- Friston KJ, Fletcher P, Josephs O, Holmes A, Rugg MD, Turner R. Event-related fMRI: characterizing differential responses. *Neuroimage* 1998;7:30–40.
- Friston KJ, Harrison L, Penny W. Dynamic causal modelling. *Neuroimage* 2003;19:1273–302.
- Friston KJ, Holmes AP, Poline JB, Grasby PJ, Williams SC, Frackowiak RS, et al. Analysis of fMRI time-series revisited. *Neuroimage* 1995;2:45–53.
- Handwerker DA, Ollinger JM, D'Esposito M. Variation of BOLD hemodynamic responses across subjects and brain regions and their effects on statistical analyses. *Neuroimage* 2004;21:1639–51.
- Hernandez L, Badre D, Noll D, Jonides J. Temporal sensitivity of event-related fMRI. *Neuroimage* 2002;17:1018–26.
- Hulsmann E, Erb M, Grodd W. From will to action: sequential cerebellar contributions to voluntary movement. *Neuroimage* 2003;20:1485–92.
- Kiebel SJ, Friston KJ. Statistical parametric mapping for event-related potentials (II): a hierarchical temporal model. *Neuroimage* 2004a;22:503–20.
- Kiebel SJ, Friston KJ. Statistical parametric mapping for event-related potentials. I. Generic considerations. *Neuroimage* 2004b;22:492–502.
- Kilner JM, Kiebel SJ, Friston KJ. Applications of random field theory to electrophysiology. *Neurosci Lett* 2005;374:174–8.
- Lamm C, Windischberger C, Leodolter U, Moser E, Bauer H. Evidence for premotor cortex activity during dynamic visuospatial imagery from single-trial functional magnetic resonance imaging and event-related slow cortical potentials. *Neuroimage* 2001;14:268–83.
- Lee AT, Glover GH, Meyer CH. Discrimination of large venous vessels in time-course spiral blood-oxygen-level-dependent magnetic-resonance functional neuroimaging. *Magn Reson Med* 1995;33:745–54.
- Lee KM, Chang KH, Roh JK. Subregions within the supplementary motor area activated at different stages of movement preparation and execution. *Neuroimage* 1999;9:117–23.
- Menon RS, Luknowsky DC, Gati JS. Mental chronometry using latency-resolved functional MRI. *Proc Natl Acad Sci USA* 1998;95:10902–7.
- Nagai Y, Critchley HD, Featherstone E, Fenwick PB, Trimble MR, Dolan RJ. Brain activity relating to the contingent negative variation: an fMRI investigation. *Neuroimage* 2004;21:1232–41.
- Oldfield RC. The assessment and analysis of handedness: the Edinburgh inventory. *Neuropsychologia* 1971;9:97–113.
- Ollinger JM, Corbetta M, Shulman GL. Separating processes within a trial in event-related functional MRI. *Neuroimage* 2001a;13:218–29.
- Ollinger JM, Shulman GL, Corbetta M. Separating processes within a trial in event-related functional MRI. *Neuroimage* 2001b;13:210–7.
- Richter W, Somorjai R, Summers R, Jarmasz M, Menon RS, Gati JS, et al. Motor area activity during mental rotation studied by time-resolved single-trial fMRI. *J Cogn Neurosci* 2000;12:310–20.
- Richter W, Ugurbil K, Georgopoulos A, Kim SG. Time-resolved fMRI of mental rotation. *Neuroreport* 1997;8:3697–702.
- Tagaris GA, Richter W, Kim SG, Pellizzer G, Andersen P, Ugurbil K, et al. Functional magnetic resonance imaging of mental rotation and memory scanning: a multidimensional scaling analysis of brain activation patterns. *Brain Res Brain Res Rev* 1998;26:106–12.
- Weilke F, Spiegel S, Boecker H, von Einsiedel HG, Conrad B, Schwaiger M, et al. Time-resolved fMRI of activation patterns in M1 and SMA during complex voluntary movement. *J Neurophysiol* 2001;85:1858–63.

- Wildgruber D, Erb M, Klose U, Grodd W. Sequential activation of supplementary motor area and primary motor cortex during self-paced finger movement in human evaluated by functional MRI. *Neurosci Lett* 1997;227:161–4.
- Wildgruber D, Pihan H, Ackermann H, Erb M, Grodd W. Dynamic brain activation during processing of emotional intonation: influence of acoustic parameters, emotional valence, and sex. *Neuroimage* 2002;15:856–69.
- Windischberger C, Lamm C, Bauer H, Moser E. Human motor cortex activity during mental rotation. *Neuroimage* 2003;20:225–32.
- Worsley K, Marrett S, Neelin P, Vandal AC, Friston KJ, Evans AC. A unified statistical approach for determining significant signals in images of cerebral activation. *Hum Brain Mapp* 1996;4:58–73.
- Worsley KJ, Andermann M, Koulis T, MacDonald D, Evans AC. Detecting changes in nonisotropic images. *Hum Brain Mapp* 1999;8:98–101.